

Adsorption of toluene vapours on micro–meso hierarchical porous carbon

Xi Yan^{1,2} ✉, Fang Liu², Guiqin Mu¹, Zhiguo Zhou¹, Yan Xie¹, Long Li¹, Yangyang Yang¹, Xinzhe Wang¹

¹SINOPEC Safety Engineering Institute, State Key Laboratory of Safety and Control for Chemicals, Qingdao 266071, People's Republic of China

²College of Chemical Engineering, China University of Petroleum, Qingdao 266580, People's Republic of China

✉ E-mail: yanxi19911024@163.com

Published in Micro & Nano Letters; Received on 30th October 2017; Revised on 15th January 2018; Accepted on 18th January 2018

This work reports the synthesis of micro–meso hierarchical porous carbons prepared with sucrose as a carbon source. With properties characterised, dynamic adsorption performances of toluene on carbons were investigated at various initial concentrations. Results showed that adsorption capacities as high as 687.60 mg/g toluene/1 cm modified carbon can be achieved. Thus, large surface area, large volume of narrow microporosity and proper average pore size are the desired parameters to achieve strong toluene adsorption capacities. Moderate amounts of surface oxygen groups can also improve the adsorbents performance.

1. Introduction: Volatile organic compounds (VOCs) such as toluene have attracted intensive attention for their toxicity, carcinogenicity, diffusivity and flammability. Their existence even at low concentrations in the atmosphere poses harm to environmental and human health [1]. With industrial developments, the increasing emission of VOCs, which causes serious air pollution, is calling for efficient methods to remove VOCs from industrial emission streams. A variety of technologies concerning VOCs removal have been proposed, such as adsorption, thermal oxidation, catalytic oxidation, biological treatment, photocatalytic oxidation and condensation [2, 3]. Among them, adsorption process is the most effective and of low cost [4, 5].

Adsorbents play important roles in the adsorption process. Porous materials with high surface area can be applied as adsorbents, such as activated carbon (AC) [6], mesoporous silica [7], zeolites [8], metal organic frameworks [9], activated carbon fibre [10] and silica gel [11]. AC has been considered to be the most extensively used adsorbent due to its high surface area, well-developed pore structure and abundant surface functional groups [12, 13], but it can only be effective for adsorbing small molecules with formula weight between 45 and 130 [14]. Mesoporous silica (MCM-41) has amorphous mesoporous walls and poor thermal and hydrothermal stabilities, which go against adsorption performance [15]. Moreover, silica gel, as an ideal desiccant, may not be expected as an appropriate adsorbent for its surface polarity. Hence, it is imperative to develop efficient adsorbents for VOCs removal.

In this Letter, micro–meso hierarchical porous carbon was synthesised using MCM-41 as a template. The carbon prepared with sucrose as a carbon source was named as MC-1. Like traditional AC, the obtained carbons have high surface area, but the pore structure, pore size distribution and surface functional groups are different, thus can be applied to adsorb both small and macro molecules. Although toluene has been considered to be one kind of typical VOC in the industry, toluene adsorption performances of MC-1 have been evaluated in this Letter. Also, the relationship between pore structure of modified carbon and toluene adsorption capacity is illustrated.

2. Experiment

2.1. Materials: Degassed mesoporous molecular sieve MCM-41 (Nankai University Catalyst Factory) was used as a template. Sucrose was used as a carbon precursor for carbon synthesis, and the product was named as MC-1. Toluene (Sinopharm Chemical Reagent Corporation, analytical grade) was used as an adsorbate to investigate the carbon adsorption performance.

2.2. Synthesis

2.2.1. Preparation of MC-1: The synthesis process of MC-1 is presented in Fig. 1. The degassed MCM-41 was impregnated with aqueous solution containing 1.25 g of sucrose, 0.14 g of H₂SO₄ and 6.0 g of H₂O. After being stirred vigorously for 24 h under room temperature, the mixture was firstly dried at 60°C for 6 h, and then dried for 6 h at 160°C. The obtained material was again mixed with aqueous solution containing 0.8 g of sucrose, 0.09 g of H₂SO₄ and 5.0 g of H₂O. After the same drying process, the mixture was calcined at 900°C for 2 h and then cooled down to room temperature under nitrogen atmosphere protection. Finally, the silica–carbon composite was stirred vigorously in NaOH (2.5 wt%) dissolved in 1:1 water–ethanol mixture [16], at least twice at 373 K.

2.2.2. Preparation of modified hierarchical porous carbon: A known amount of carbons were dried in a vacuum drying oven for at least 12 h at 110°C before further treatment. The modification was carried out using 20% w/w nitric acid solution, and the mixture was continuously stirred at 45°C for 6 h (MC-N) and 24 h (MC-N'), respectively. The suspension solutions were then washed by distilled water until neutral pH was reached. Finally, the resultant samples were dried under vacuum at 110°C, and then kept in a desiccator for later use.

2.3. Characterisation: The samples were examined by transmission electron microscopy (TEM, JEM-2100). The surface morphologies of the samples were observed by a field emission scanning electron microscope (SEM, Hitachi S-4800). Nitrogen sorption isotherms were measured with a Micromeritics ASAP 2020 at 77 K. The specific surface areas and pore volumes were calculated by the Brunauer–Emmett–Teller (BET) method. The Barrett–Joyner–Halenda (BJH) method and the Horvath–Kawazoe (HK) method were applied to analyse meso- and micropore size distributions, respectively. The micropore surface areas were measured by the slopes from the t-plot method. Infrared analysis of carbons was performed on a NEXUS FTIR spectrometer.

2.4. Toluene adsorption

2.4.1. Experimental device: Adsorption experiments were carried out at a laboratory scale in a continuous flow-type adsorption system (Fig. 2), which is composed of a fixed bed reactor (inner diameter: 20 mm; length: 250 mm) and a gas mixing apparatus. Air was introduced into the system by air pump. The toluene vapour flow was generated by bubbling toluene liquid in the

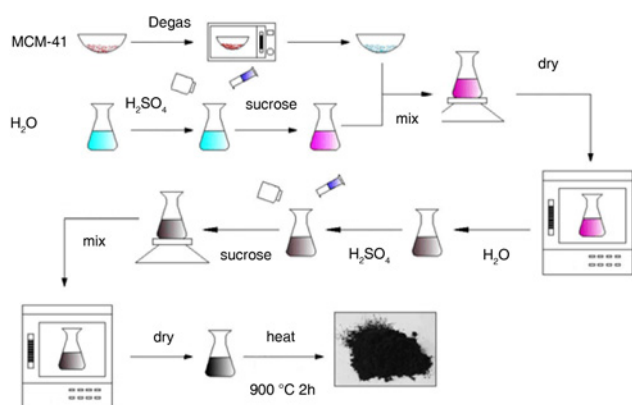


Fig. 1 Synthesis process of MC-1

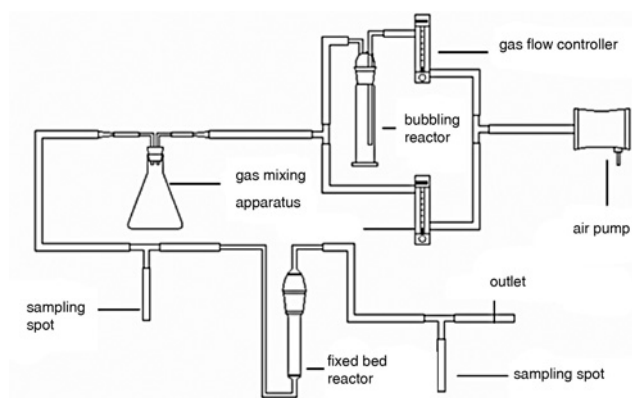


Fig. 2 Toluene adsorption experimental device

reactor. The concentration of toluene (1750 mg/m^3) was acquired by adjusting the appropriate air flow rate. A 100 ml glass injectors, which were connected to sampling spots, were used to collect gas samples before and after the adsorption treatment.

2.4.2. Experimental methods: The toluene adsorption experiments on 1 cm adsorbents (MC-1, MC-2, MC-3, MC-N and MCM-41) were performed at 25°C . The concentrations of toluene were controlled in the range between 389 and 3869 mg/m^3 . Prior to use, all the adsorbents were dehydrated under vacuum overnight at high temperature. The inlet and outlet toluene concentrations were determined by gas chromatography (SP-3420A). The adsorption curves can be obtained through plotting toluene outlet concentrations versus time. In the adsorption curve, the breakthrough time was defined when the output concentration (C) reached 10% of the inlet concentration (C_0) (min), and the saturation time was defined when the output concentration (C) reached 95% of the inlet concentration (C_0) (min). Column weights were measured before and after saturation, thus the toluene adsorption capacity (q_c) of each adsorbent can be calculated as follows:

$$q_c = \frac{m_e - m_0}{m_0} \quad (1)$$

where m_0 (mg) and m_e (mg) were the mass of the initial and saturated adsorption columns, respectively.

2.5. Correlation analysis: Before analysis, MC-1, MC-N and MC-N' were degassed in a 110°C vacuum oven for at least 12 h. The toluene adsorption experiments on degassed adsorbents (MC-1, MC-N, MC-N') were carried out when the toluene concentration was 1750 mg/m^3 and the temperature was 25°C . Then the relationship between pore structure parameters (specific surface

area, pore volume) and toluene adsorption capacity was analysed by combining experimental results and mathematical methods.

3. Results and discussion

3.1. Carbon properties: The scanning electron microscope images of carbons are shown in Fig. 3. It shows that all the carbons possess layered and porous structure. MC-1 has pit-like micropore structure in Fig. 3a. There is little difference in the surface morphology of MC-1 and MC-N, except for some apparent pore widening on MC-N. This may due to the fact that the pore structure was eroded during the oxidation process [17]. Fig. 4 displays the TEM images of MC-1 and MC-N. Both MC-1 and MC-N possess a non-uniform pore distribution.

The nitrogen adsorption–desorption isotherms obtained from the carbons are shown in Fig. 5. Table 1 summarises BET surface areas and volumes of total pore as well as micropore. According to IUPAC classification [18], the curves display a typical type-IV

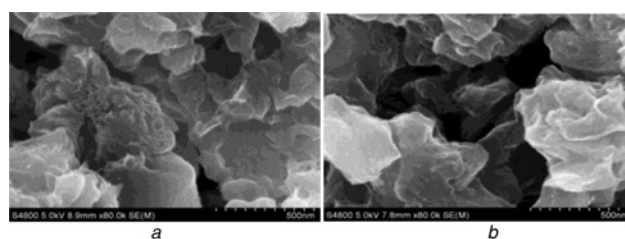


Fig. 3 Scanning electron microscope images of adsorbents
a MC-1 magnification $\times 80.0\text{k}$
b MC-N magnification $\times 80.0\text{k}$

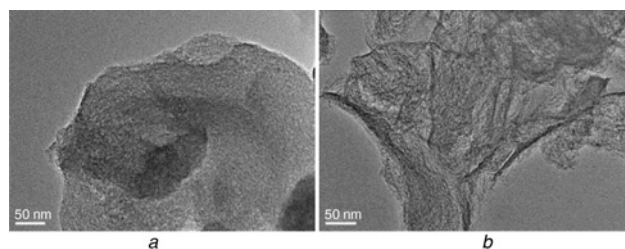


Fig. 4 Transmission electron microscope images of carbons
a MC-1
b MC-N

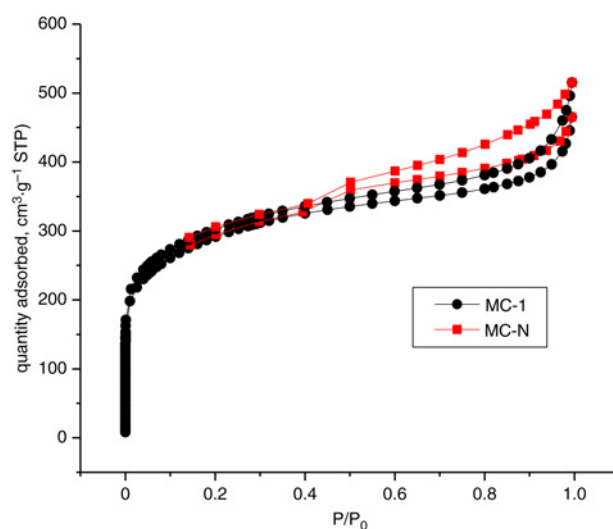


Fig. 5 Nitrogen adsorption–desorption isotherms at 77 K for MC-1 and MC-N

Table 1 Properties of adsorbents

	MCM-41	MC-1	MC-N
S_{BET} , m ² /g	1043	1052.44	1104.08
V_{total} , cm ³ /g	0.91	0.52	0.58
pore diameter, nm	2.86	4.08	4.6
S_{mic} , m ² /g	0	950.28	994.6826
V_{mic} , cm ³ /g	0	0.47	0.52

isotherm with a H4 hysteresis loop. The curves indicate that MC-1 have a wide pore size distribution. The abrupt rise of the curves at low relative pressure reveals the largely microporous nature of the carbons [19, 20]. Then there is a gradual increase in the curves for the existence of mesopores, the H4 hysteresis cycle is also indicative of the presence of mesopores [21]. It can be observed that HNO₃ modification of the carbon resulted in the increase in the BET surface area and the mesopore volume. Increase in BET surface area is attributable to increase in micropore volume [22]. This is as a result of fresh micropore formation caused by reaction between nitric acid and surface impurities. This observation can also be attributed to the fact that the pore blockage was opened by reaction gas.

Fig. 6 depicts the pore size distribution of MC-1 and MC-N. MC-1 possesses rich amount of micropores (with peaks

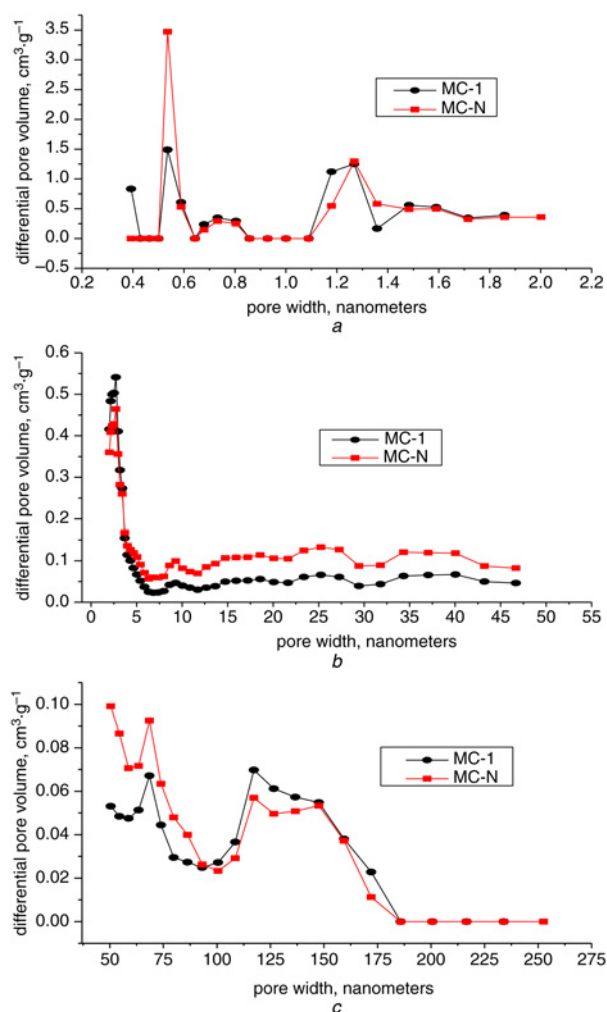


Fig. 6 Pore size distribution of MC-1 and MC-N
 a Micropore volume distribution
 b Mesopore volume distribution
 c Macropore volume distribution

around 0.5–0.6, 0.6–0.8, 1.1–1.4 and 1.4–1.7 nm). One peak appears at around 3.5 nm demonstrating the existence of mesopore. The micropores of MC-N had a multimodal distribution, which was centred between 0.5–0.8, 0.6–0.8 and 1.4–2 nm, with peaks around 0.52 and 1.28 nm. It can be observed that the V_{mic} of MC-N is much higher than that of MC-1. One peak exists in mesopore distribution, at around 3.5 nm. The macropores of MC-N exhibited bimodal distributions, including peaks at around 75 and 125 nm.

IR spectra of the carbons are depicted in Fig. 7. Some similarities can be observed from the spectral of MC-1 and MC-N, which indicates that MC-N have similar surface groups with MC-1. The peaks exist at 797 and 693 cm⁻¹ can be attributed to C–H bending vibrations. A strong peak can be observed at 1000–1250 cm⁻¹, which can be attributed to C–O stretching vibrations. The peak at 1500–1650 cm⁻¹ can be assigned to –COOH group vibrations [23, 24]. There is a peak of transmittance that exist at 3200–3670 cm⁻¹, and it can be ascribed to O–H stretching [25, 26]. The more pronounced peaks at 1000–1250, 1500–1650 and 3200–3670 cm⁻¹ imply that there is more oxygen-containing groups in the MC-N sample than in the MC-1 sample. The new peaks of MC-N that exist at 1050–1020 cm⁻¹ can be attributed to C–N bending vibrations.

3.2. Toluene adsorption isotherms

3.2.1. Toluene adsorption curves under different initial concentrations: Fig. 8 is obtained by allowing diluted toluene gas at 200 ml/min to flow through a column where 1 cm adsorbents are packed. The adsorption experiments are conducted at 25°C, while the initial concentration of toluene (C_0) varied from 389 to

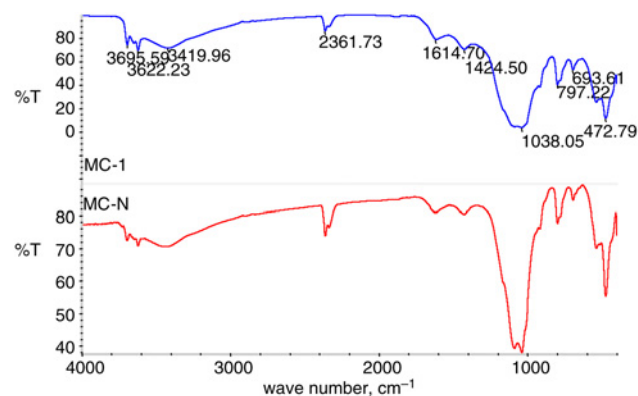


Fig. 7 IR spectra of MC-1 and MC-N

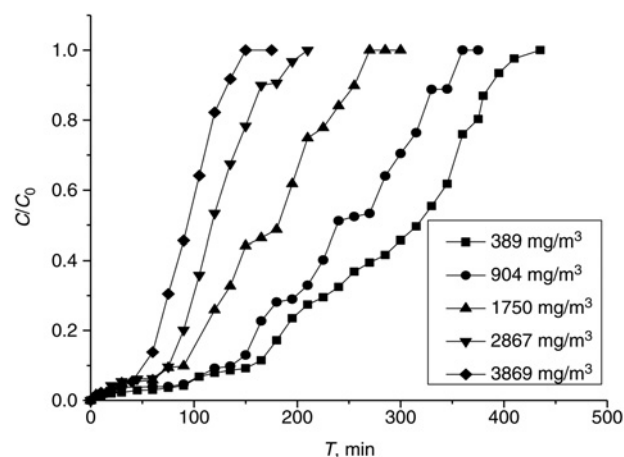


Fig. 8 Toluene adsorption isotherms on MC-1 under different initial concentrations

3869 mg/m³. The toluene adsorption parameters onto MC-1 are listed in Table 2. It can be observed that the adsorption curves have identical curvilinear trend. From Fig. 8, there is a gradual increase of the curves at the beginning, for the abundant micropores of carbons are beneficial to toluene adsorption capacity [27, 28]. Then, the increase becomes more rapid after the breakthrough point ($C/C_0=0.1$), and this may be due to the fact that the filling of the microporosity in the carbons nearly approached completion. This suggests that the large amount of adsorbed toluene may lead to minor toluene adsorption capacity. With the decrease of toluene initial concentration, the saturation time of carbons becomes longer. This may be due to the fact that when the initial concentration becomes lower, the mass transfer resistance is lower, which can improve the internal diffusion coefficient of toluene molecules in the carbons [29, 30].

3.2.2. Equation fitting curves: Fig. 9 clearly shows that the experimental data can be well described by both the Langmuir equation and the Freundlich equation. The equation relative parameters were calculated by linear regression fitting, and listed in Table 3. From Fig. 9 and Table 3, it can be observed that the correlation coefficients (R^2) value of Langmuir equation is larger than that of the Freundlich equation, indicating that the Langmuir equation

Table 2 Toluene adsorption parameters onto MC-1 at different concentrations

Initial concentrations, mg/m ³	Breakthrough time, min	Saturation time, min	Toluene adsorbed amount, mg/g
389	155	401	94.1
904	136	362	165.7
1750	91	269	185.3
2867	76	187	232.5
3869	51	141	264.7

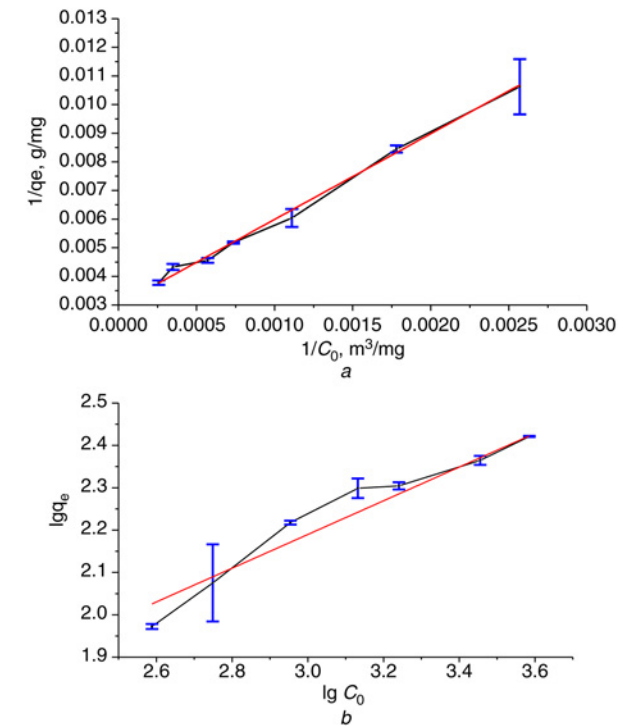


Fig. 9 Equation fitting curves
a Langmuir equation fitting curve
b Freundlich equation fitting curve

can better describe the experimental data. This represents that the adsorption process on the adsorbents is mainly single molecular layer adsorption via physical method [31].

3.3. Correlation analysis: In order to analyse the relationship between the adsorption capacity and the pore structure of the carbon samples, adsorption experiments were carried out by allowing diluted toluene (1750 mg/m³) gas at 200 ml/min at 25°C to flow through a column where 10 mm adsorbents (MC-1, MC-N and MC-N') were packed. The modification conditions of MC-N' are nitric acid concentrate 20%, modification time 24 h and temperature 45°C.

Fig. 10 shows the significant linear relationship between the specific surface area and the adsorption capacity. There is a significant linear relationship between the adsorption capacity of toluene and the surface area. The coefficients of relation are 0.8479 (S_{BET}) and 0.8626 (S_{mic}), respectively. The correlation between the adsorption capacities of toluene and pore volumes has also been studied in carbon samples. Fig. 10 shows that good relationship is found when correlating the toluene adsorption capacity with the pore volume of micropore. The coefficients of relation are 0.9389 (V_{BET}) and 0.999

Table 3 Relative parameters of Langmuir equation and Freundlich equation

Langmuir				Freundlich			
q_m	K_L	R^2	RSS	n	K_F	R^2	RSS
333.3	0.001	0.99	1.83×10^{-7}	2.33	7.08	0.94	0.007

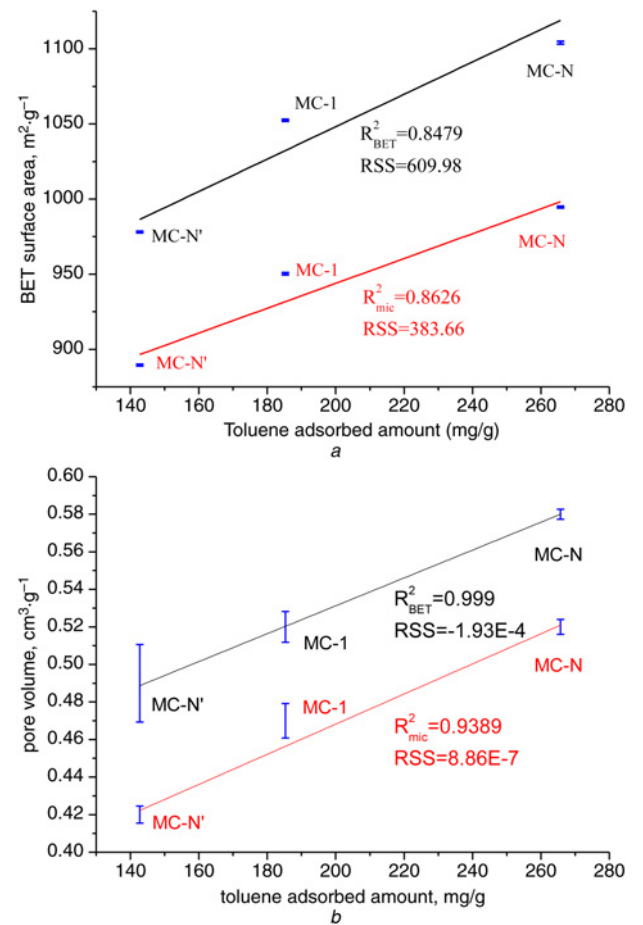


Fig. 10 Relationship between pore structure and adsorption capacity
a Relationship between surface area and adsorption capacity
b Relationship between pore volume and adsorption capacity

(V_{mic}), respectively. According to the coefficients of relation (R^2), the descending order of the importance of each factor is as follows: total pore volume>micropore volume>surface area of micropores>surface area. The results indicate that the BET surface area and micropore content are the two factors that must be considered to optimise the adsorbents performance.

4. Conclusion: In order to diminish the effects of refractory organic gas on the environment, this Letter has analysed the synthesis of micro-meso hierarchical porous carbon and their application to toluene adsorption. The carbons are synthesised using MCM-41 as a hard-template and sucrose as a carbon source. The results show that an excellent toluene adsorption capacity of 185.30 mg/g (MC-1) can be achieved, and the toluene adsorption capacity increased to 687.60 mg/g (MC-N) when using nitric acid as a modifier. Thus, two important factors affecting the toluene adsorption capacity are studied: the porosity and the surface oxygen groups. The result also shows that the large surface area and the proper average pore size are the desired parameters to achieve strong toluene adsorption capacities. Then further experiments are carried out to investigate the relationship between the pore structure and the toluene adsorption capacity. According to the coefficients of relation (R^2), the descending order of the importance of each factor is as follows: total pore volume>micropore volume>surface area of micropores>surface area, which allows us to conclude that when enlarging the volume of smaller micropores (<0.7 nm), the adsorbents have higher adsorption capacity. Besides, the surface chemistry of carbon has a significant effect on the uptake of toluene molecules, thus the content in surface oxygen groups also seems to be one of the most important parameters affecting the performance of adsorbents. The data obtained were correlated with both the Langmuir equation and the Freundlich equation, and the Langmuir equation leads to a better correlation of the experimental data, which represents that the adsorption process on the adsorbents is mainly single molecular layer adsorption via physical method. From a practical point of view, the porosity and the surface oxygen groups are the two factors that must be considered for optimisation in order to obtain high-performance adsorbents.

5. Acknowledgment: This research was supported by the Ministry of Science and Technology of the People's Republic of China through grant no. 2016YFC1402406.

6 References

- [1] Lillo-Rodenas M.A., Cazorla-Amoros D., Linares-Solano A.: 'Behaviour of activated carbons with different pore size distributions and surface oxygen groups for benzene and toluene adsorption at low concentrations', *Carbon*, 2005, **43**, pp. 1758–1767
- [2] Bouazza N., Lillo-Rodenas M.A., Linares-Solano A.: 'Photocatalytic activity of TiO₂-based materials for the oxidation of propene and benzene at low concentration in presence of humidity', *Appl. Catal. B: Environ.*, 2008, **84**, pp. 691–698
- [3] Hort C., Gracy S., Platel V., *ET AL.*: 'Evaluation of sewage sludge and yard waste compost as a biofilter media for the removal of ammonia and volatile organic sulfur compounds (VOSCs)', *Chem. Eng. J.*, 2009, **152**, pp. 44–53
- [4] Romero-Anaya A.J., Lillo-Rodenas M.A., Linares-Solano A.: 'Spherical activated carbons for low concentration toluene adsorption', *Carbon*, 2010, **48**, (9), pp. 2625–2633
- [5] Fletcher A.J., Yu Z.Y., Thomas K.M.: 'Adsorption and desorption kinetics for hydrophilic and hydrophobic vapors on activated carbon', *Carbon*, 2006, **44**, pp. 989–1004
- [6] Wibowo N., Setyadhi L., Wibowo D., *ET AL.*: 'Adsorption of benzene and toluene from aqueous solutions onto activated carbon and its acid and heat treated forms: influence of surface chemistry on adsorption', *J. Hazard. Mater.*, 2007, **146**, (1–2), pp. 237–242
- [7] Serna-Guerrero R., Sayari A.: 'Applications of pore-expanded mesoporous silica. Adsorption of volatile organic compounds', *Environ. Sci. Technol.*, 2007, **41**, pp. 4761–4766
- [8] Lee D.-G., Kim J.-H., Lee C.-H.: 'Adsorption and thermal regeneration of acetone and toluene vapors in dealuminated Y-zeolite bed', *Sep. Purif. Technol.*, 2011, **77**, pp. 312–324
- [9] Huang C.-Y., Song M., Gu Z.-Y., *ET AL.*: 'Probing the adsorption characteristic of metal-organic framework MIL-101 for volatile organic compounds by quartz crystal microbalance', *Environ. Sci. Technol.*, 2011, **45**, pp. 4490–4496
- [10] Liu Z.-H., Qiu J.-R., Liu H., *ET AL.*: 'Effects of SO₂ and NO on removal of VOCs from simulated flue gas by using activated carbon fibers at low temperatures', *J. Fuel Chem. Technol.*, 2012, **40**, pp. 93–99
- [11] Chen X.T., Quan Y., Wang Y., *ET AL.*: 'Treatment of uranium-containing process wastewater with high concentration nitrate by silica gel adsorption method', *Yuanzheneng Kexue Jishu/Atomic Energy Sci. Technol.*, 2014, **48**, (11), pp. 1928–1932
- [12] Chingombe P., Saha B., Wakeman R.J.: 'Surface modification and characterisation of a coal-based activated carbon', *Carbon*, 2005, **43**, (15), pp. 3132–3143
- [13] Yu C., Qiu J.S., Sun Y.F., *ET AL.*: 'Adsorption removal of thiophene and dibenzothiophene from oils with activated carbon as adsorbent: effect of surface chemistry', *J. Porous Mater.*, 2008, **15**, (2), pp. 151–157
- [14] Dolidovich A.F., Akhremkova G.S., Efremtsev V.S.: 'Novel technologies of VOC decontamination in fixed, moving and fluidized catalyst-adsorbent beds', *Can. J. Chem. Eng. Sci.*, 1999, **77**, p. 342
- [15] Mody H.M., Kannan S., Bajaj H.C., *ET AL.*: 'A simple room temperature synthesis of MCM-41 with enhanced thermal and hydrothermal stability', *J. Porous Mater.*, 2008, **15**, p. 571
- [16] Ryoo R., Joo S.H., Kim J.M.: 'Energetically favored formation of MCM-48 from cationic – neutral surfactant mixtures', *Phys. Chem. B*, 1999, **103**, (35), pp. 7435–7440
- [17] Chingombe P., Saha B., Wakeman R.J.: 'Surface modification and characterization of a coal-based activated carbon', *Carbon*, 2005, **43**, (43), pp. 3132–3143
- [18] Gregg S.J., Sing K.S.W.: 'Adsorption, surface area and porosity' (Academic Press, London, 1986)
- [19] Lo A.-Y., Hung C.-T., Yu N., *ET AL.*: 'Syntheses of carbon porous materials with varied pore sizes and their performances as catalyst supports during methanol oxidation reaction', *Clean Energy Future Gener.*, 2012, **100**, pp. 66–74
- [20] Wibowo N., Setyadhi L., Wibowo D., *ET AL.*: 'Adsorption of benzene and toluene from aqueous solutions onto activated carbon and its acid and heat treated forms: influence of surface chemistry on adsorption', *J. Hazard. Mater.*, 2007, **146**, pp. 237–242
- [21] Payer K.R., Hammond K.D., Tompsett G.A., *ET AL.*: 'The effects of mechanical and thermal perturbations on states within the hysteresis of sorption isotherms of mesoporous materials', *J. Porous Mater.*, 2009, **16**, (1), pp. 91–99
- [22] Li L., Quinlivan P.A., Knappe D.R.U.: 'Effects of activated carbon surface chemistry and pore structure on the adsorption of organic contaminants from aqueous solution', *Carbon*, 2002, **40**, pp. 2085–2100
- [23] Adib F., Bagreev A., Bandosz T.J.: 'Analysis of the relationship between H₂S removal capacity and surface properties of unimpregnated activated carbons', *Environ. Sci. Technol.*, 2000, **34**, (4), pp. 686–692
- [24] Schepetkin A.I., Khlebnikov I.A., Ah Y.S., *ET AL.*: 'Characterization and biological activities of humic substances from mumie', *J. Agric. Food Chem.*, 2003, **51**, pp. 5245–5254
- [25] Chen P.J., Wu S.: 'Acid/base-treated carbons: characterization of functional groups and metal adsorption properties', *Langmuir*, 2004, **20**, pp. 233–242
- [26] Zhu T., Ertekin E.: 'Generalized Debye-Peierls/Allen-Feldman model for the lattice thermal conductivity of low-dimensional and disordered materials', *Phys. Rev. B*, 2016, **93**, (15), pp. 1–13
- [27] Song Y., Qiao W.M., Yoon S.-H., *ET AL.*: 'Toluene adsorption on various activated carbons with different pore structures', *New Carbon Mater.*, 2005, **12**, (20), pp. 294–298
- [28] Ranganathan R., Rokkam S., Desai T., *ET AL.*: 'Generation of amorphous carbon models using liquid quench method: a reactive molecular dynamics study', *Carbon*, 2017, **113**, pp. 87–99
- [29] Mohana N., Kannana G.K., Upendra S., *ET AL.*: 'Breakthrough of toluene vapours in granular activated carbon filled packed bed reactor', *J. Hazard. Mater.*, 2009, **168**, (2/3), pp. 777–781
- [30] Zhu T., Ertekin E.: 'Phonons, localization, and thermal conductivity of diamond nanowires and amorphous graphene', *Nano Lett.*, 2016, **16**, (8), pp. 4763–4772
- [31] Fytianos K., Voudrias E., Kokkalis E.: 'Sorption-desorption behavior of 2, 4-dichlorophenol by marine sediments', *Chemosphere*, 2000, **40**, (6), pp. 3–6